(Fig. 2C, red symbols). We thus conclude that charge interaction is responsible for confinement of the protein.

Immobilization may be unfavorable because of steric effects or because proteins are not point charges. Our experiments show that molecules do not have to be physically immobilized to be chromatographically retained. Trapping is found in a thick zone where molecular behavior is intermediate between bulk and surface regimes. The large distances involved cannot be explained by the Derjaguin-Landau-Verwey-Overbeek theory (*27*) for interactions between charged surfaces across liquids, even in the regime of reduced charge densities (*28*). Long-range attractive interaction has been reported for polystyrene sulfonate spheres near a charged glass surface (*29*). The distances (50 nm if scaled to our ionic strengths) are comparable with those here, although metastable colloidal crystallites may not properly model proteins. It may well be that restricted motion of the counter ions near the surface (*11*) lowers the efficiency of electrostatic shielding to extend the interaction distance. This implies that the interaction of protein molecules with biological cell surfaces can be much more efficient than predicted by random diffusion, which in turn enhances binding to receptors. Although here we relied on the inherent surface charge on fused silica to follow one type of protein retention, other interactions can be studied by coating chromatographic materials, creating self-assembled monolayers, or attaching actual cell membranes on the solid surface.

References and Notes

1. J. T. Petty *et al*., *Anal. Chem.* **67**, 1755 (1995).
2. S. Nie, D. T. Chiu, R. N. Zare, *Science* **266**, 1018 (1994).
3. _____, *Anal. Chem.* **67**, 2849 (1995).
4. M. Eigen and R. Rigler, *Proc. Natl. Acad. Sci. U.S.A.* **91**, 5740 (1994).
5. Q. Xue and E. S. Yeung, *Nature* **373**, 681 (1995).
6. W. Tan and E. S. Yeung, *Anal. Chem.* **69**, 4242 (1997).
7. D. B. Craig, E. A. Arriaga, J. C. Y. Wong, H. Lu, N. J. Dovichi, *J. Am. Chem. Soc.* **118**, 5245 (1996).
8. T. Schmidt, G. J. Schutz, W. Baumgartner, H. J. Gruber, H. Schindler, *Proc. Natl. Acad. Sci. U.S.A.* **93**, 2926 (1996).
9. R. M. Dickson, D. J. Norris, Y.-L. Tzeng, W. E. Moerner, *Science* **274**, 966 (1996).
10. T. Funatsu, Y. Harada, M. Tokunaga, K. Saito, T. Yanagida, *Nature* **374**, 555 (1995).
11. X.-H. Xu and E. S. Yeung, *Science* **275**, 1106 (1997).
12. These represent relative counts and not absolute counts, because the ICCD detection threshold was set artificially high to eliminate all false-positive events that would have distorted the accompanying measurements of spot sizes and to avoid artifacts due to photobleaching. Only the most extensively labeled molecules in the sample population can exceed the detection threshold. Their behavior is still representative because a neutral label is used.
13. J. C. Reijenga, G. V. A. Aben, Th. P. E. M. Verheggen, F. M. Everaerts, *J. Chromatogr.* **260**, 241 (1983).
14. W. J. Lambert and D. L. Middleton, *Anal. Chem.* **62**, 1585 (1990).
15. A. J. Bard and L. R. Faulkner, *Electrochemical Methods, Fundamentals and Applications* (Wiley, New York, 1980), pp. 488–510.
16. J. O'M. Bockris and A. K. N. Reddy, *Modern Electrochemistry* (Plenum, New York, 1970), vol. 2, pp. 826–841.
17. C. Gutierrez and C. Melendres, Eds., *Spectroscopic and Diffraction Techniques in Interfacial Electrochemistry* (Kluwer Academic, Boston, 1990), pp. 1–469.
18. J. Lipkowski and P. N. Ross, Eds., *Structure of Electrified Interfaces* (VCH, New York, 1993), p. 201 and p. 277.
19. T. S. Stevens and H. J. Cortes, *Anal. Chem.* **55**, 1365 (1983).
20. M. Martin and G. Guiochon, *ibid.* **56**, 614 (1984).
21. N. Iki, Y. Kim, E. S. Yeung, *ibid.* **68**, 4321 (1996).
22. J. Roeraade, Abstract WL-11-4, Eighth International Symposium on High Performance Capillary Electrophoresis, Orlando, FL, January 1996.
23. W. A. Lyon and S. Nie, *Anal. Chem.* **69**, 3400 (1997).
24. C. L. Rice and R. Whitehead, *J. Phys. Chem.* **69**, 4017 (1965).
25. D. A. Skoog and J. J. Leary, *Principles of Instrumental Analysis* (Saunders, New York, ed. 4, 1992), pp. 579–601.
26. F. E. P. Mikkers, F. M. Everaerts, Th. P. E. M. Verheggen, *J. Chromatogr.* **169**, 11 (1979).
27. B. V. Derjaguin and L. Landau, *Acta Physicochim. U.S.S.R.* **14**, 633 (1941); E. J. W. Verwey and J. Th. G. Overbeek, *Theory of the Stability of Lyophobic Colloids* (Elsevier, Amsterdam, 1948).
28. S. H. Behrens, M. Borkovec, P. Schurtenberger, *Langmuir* **14**, 1951 (1998). There, a secondary minimum is predicted as a result of the interplay between charge repulsion and van der Waals attraction. However, that feature is more prominent toward higher ionic strengths, in variance with our observations of enhanced trapping toward lower ionic strengths.
29. A. E. Larsen and D. G. Grier, *Nature* **385**, 230 (1997).

30. The Ames Laboratory is operated for the U.S. Department of Energy by Iowa State University under contract number W-7405-Eng-82. Supported by the Director of Energy Research, Office of Basic Energy Sciences, Division of Chemical Sciences.

26 January 1998; accepted 3 August 1998

Design of Organic Molecules with Large Two-Photon Absorption Cross Sections

Marius Albota, David Beljonne, Jean-Luc Brédas,* Jeffrey E. Ehrlich, Jia-Ying Fu, Ahmed A. Heikal, Samuel E. Hess, Thierry Kogej, Michael D. Levin, Seth R. Marder,* Dianne McCord-Maughon, Joseph W. Perry,* Harald Röckel, Mariacristina Rumi, Girija Subramaniam, Watt W. Webb,* Xiang-Li Wu, Chris Xu

A strategy for the design of molecules with large two-photon absorption cross sections, δ, was developed, on the basis of the concept that symmetric charge transfer, from the ends of a conjugated system to the middle, or vice versa, upon excitation is correlated to enhanced values of δ. Synthesized bis(styryl)benzene derivatives with donor-π-donor, donor-acceptor-donor, and acceptor-donor-acceptor structural motifs exhibit exceptionally large values of δ, up to about 400 times that of *trans*-stilbene. Quantum chemical calculations performed on these molecules indicate that substantial symmetric charge redistribution occurs upon excitation and provide δ values in good agreement with experimental values. The combination of large δ and high fluorescence quantum yield or triplet yield exhibited by molecules developed here offers potential for unprecedented brightness in two-photon fluorescent imaging or enhanced photosensitivity in two-photon sensitization, respectively.

In the presence of intense laser pulses, molecules can simultaneously absorb two or more photons, and the transition probability for absorption of two identical photons is proportional to I^2, where I is the intensity of the laser pulse. Molecules with a large two-photon absorption cross section, δ, are in great demand for variety of applications, including two-photon–excited fluorescence microscopy (*1*), optical limiting (*2*, *3*), three-dimensional optical data storage (*4*), and two-photon induced biological caging studies (*5*). These applications use two key features of two-photon absorption, namely, the ability to create excited states with photons of half the nominal excitation energy, which can provide improved penetration in absorbing or scattering media, and the I^2 dependence of the process, which allows for excitation of chromophores with a high degree of spatial selectivity in three dimensions through the use of a tightly focused laser beam. Unfortunately, most known organic molecules have relatively small δ, and criteria for the design of molecules with large δ have not been well developed (*6*, *7*). As a result, the full utility of two-photon–absorbing materials has not been realized. Here, we report on design strategies and structure-property studies for two-photon absorption, which resulted in the synthesis of fluorescent molecules with unprecedented δ values.

Initial optical studies revealed that 4,4′-bis(di-*n*-butylamino)-*E*-stilbene, **2** (Fig. 1), in toluene solution, exhibited a strong blue fluorescence that depended on I^2 when exposed to 5-ns laser pulses at 605 nm. Compound **2** has a linear absorption peak at 374 nm, an emission maximum at 410 nm, and a fluorescence quantum yield, Φ_f, of 0.90. The two-photon–excited fluorescence spectrum for **2** was essentially identical to that excited by one-photon absorption into S_1, suggesting that there was rapid relaxation of the state reached by two-photon absorption (taken to be S_2) to the S_1 state and subsequent fluorescence from that state. Measurement of the two-photon excitation cross section for **2** gave a maximum δ of 210×10^{-50} cm^4 s photon^{-1} at an excitation wavelength of 605 nm, which is almost 20 times greater than that of *E*-stilbene, **1** (*8*), and is among the largest values of δ reported for organic compounds. We conjectured that the large increase in the two-photon absorption for **2** relative to **1** was related to a symmetrical charge transfer from the amino nitrogen atoms to the conjugated bridge of the molecule.

To gain insight into the origin of the large δ value for **2** relative to **1**, we performed quantum chemical calculations on **1** and 4,4′-bis(dimethylamino)-*E*-stilbene. Using AM1 (*9*) optimized geometries, we calculated the energies (*E*) and transition dipole moments (*M*) for the singlet excited states of both compounds by combining the intermediate neglect of differential overlap (INDO) (*10*) Hamiltonian with the multireference double-configuration interaction (MRD-CI) (*11*) scheme. The frequency dependence of δ, δ(ω), is related to the imaginary part of the second hyperpolarizability, $Im\gamma(-\omega;\omega,\omega,-\omega)$ by (*12*)

$$\delta(\omega) = \frac{8\pi^2\hbar\omega^2}{n^2c^2} L^4 \, Im\gamma(-\omega;\, \omega,\omega,-\omega) \quad (1)$$

where $\hbar$ is Planck's constant divided by 2π, *n* is the index of refraction of the medium (vacuum assumed for the calculations), *L* is a local field factor (equal to 1 for vacuum), and *c* is the speed of light. We calculated $Im\gamma(-\omega;\omega,\omega,-\omega)$ using the sum-over-states (SOS) (*13*) expression (the damping factor Γ has been set to 0.1 eV in all cases in this study).

As can be seen in Table 1, the calculations predict roughly an order of magnitude enhancement in δ upon substitution of *trans*-stilbene with terminal dimethylamino groups, consistent with the experimental data presented above. This two-photon transition is from the ground state (S_0, $1A_g$) to the lowest excited state with A_g symmetry (S_2, $2A_g$). For both molecules, the S_2 state is located at about 0.8 eV above the lowest one-photon allowed excited state (S_1, $1B_u$) (Fig. 2). A simplified form of the SOS expression for the peak two-photon resonance value of δ(ω) for the $S_0 \rightarrow S_2$ transition, $\delta_{S_0 \rightarrow S_2}$, is

$$\delta_{S_0 \rightarrow S_2} \propto \frac{M_{01}^2 \, M_{12}^2}{(E_1 - E_0 - \hbar\omega)^2 \Gamma} \quad (2)$$

where the subscripts 0, 1, and 2 refer to S_0, S_1, and S_2 states, respectively, and $\hbar\omega = (E_2 - E_0)/2$. This expression results from taking S_1 as the dominant intermediate state and is valid when $(E_1 - E_0 - \hbar\omega)$ is large compared with the damping factor for the $S_0 \rightarrow S_1$ transition. On the basis of the results of the calculations, as shown in Fig. 2, we can rationalize the increase in $\delta_{S_0 \rightarrow S_2}$ on going from *trans*-stilbene to 4,4′-bis(dimethylamino)-*E*-stilbene on the basis of (i) an increase in the S_1 to S_2 transition dipole moment (M_{12}) from 3.1 to 7.2 D, (ii) an increase in the S_0 to S_1 transition dipole moment (M_{01}) from 7.1 to 8.8 D, and (iii) a decrease in the one-photon detuning term, $(E_1 - E_0 - \hbar\omega)$, from 1.8 to 1.5 eV. This enhancement results from the electron-donating properties of the terminal amino groups. The calculations also show that the electronic excitation from S_0 to S_1 is accompanied by a substantial charge transfer (~0.14 e) from the amino groups to the central vinylene linkage, as we had hypothesized, resulting in a large change in quadrupole moment upon excitation (a similar sense and magnitude of charge transfer are calculated for the $S_0 \rightarrow S_2$ transition). This pronounced redistribution of the π-electronic density is correlated with an increase of electron delocalization in the first excited state and results in a substantial increase in the S_1 to S_2 transition dipole moment, which is the major contributor to the enhanced δ value of 4,4′-bis(dimethylamino)-*E*-stilbene with respect to that of *trans*-stilbene. Another consequence of the terminal substitution with electron donors is a shift of the position of the two-photon resonance to lower energy.

These results suggested several strategies to enhance δ and tune the wavelength of the

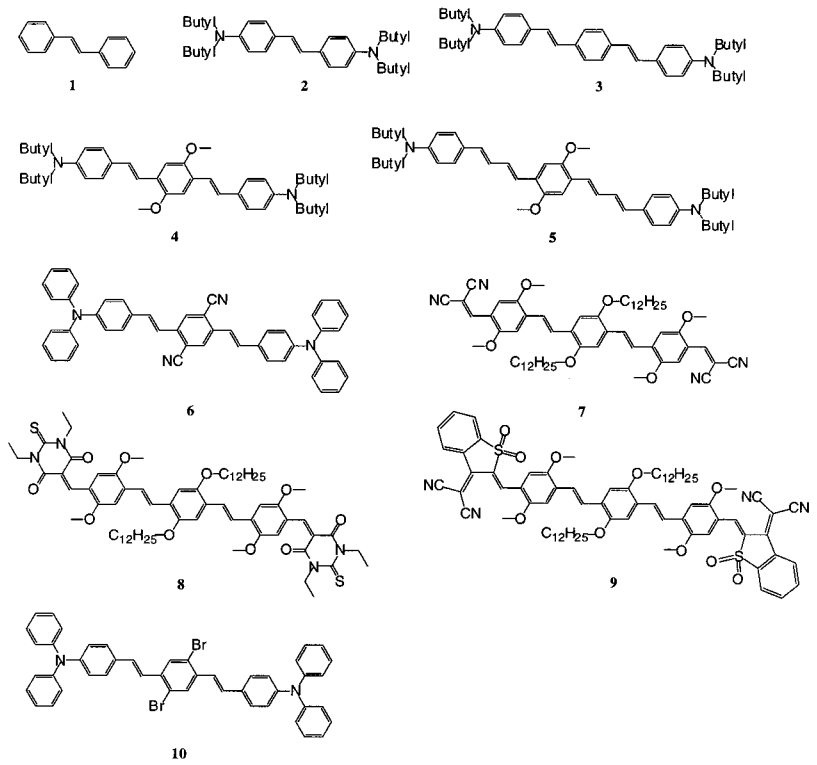

Fig. 1. Structures and numbering scheme for compounds studied in this paper.

M. Albota, S. E. Hess, W. W. Webb, C. Xu, School of Applied Physics and Engineering, and Developmental Resource for Biophysical Imaging Opto-Electronics, Cornell University, Ithaca, NY 14853, USA. D. Beljonne, J.-L. Brédas, T. Kogej, Center for Research on Molecular Electronics and Photonics, Université de Mons-Hainaut, Place du Parc 20, B-7000 Mons, Belgium. J. E. Ehrlich, Jet Propulsion Laboratory, 67-119, California Institute of Technology, Pasadena, CA 91109, USA. J.-Y. Fu, A. A. Heikal, M. Rumi, X.-L. Wu, Molecular Materials Resource Center, Beckman Institute, 139-74, California Institute of Technology, Pasadena, CA 91125, USA, and Jet Propulsion Laboratory, 67-119, California Institute of Technology, Pasadena, CA 91109, USA. M. D. Levin, D. McCord-Maughon, H. Röckel, Molecular Materials Resource Center, Beckman Institute, 139-74, California Institute of Technology, Pasadena, CA 91125, USA. S. R. Marder and J. W. Perry, Department of Chemistry, University of Arizona, Tucson, AZ 85721, USA, Molecular Materials Resource Center, Beckman Institute, 139-74, California Institute of Technology, Pasadena, CA 91125, USA, and Jet Propulsion Laboratory, 67-119, California Institute of Technology, Pasadena, CA 91109, USA. G. Subramaniam, Department of Chemistry, Pennsylvania State University, Hazleton, PA 18201, USA.

*To whom correspondence should be addressed.

two-photon absorption peak for π-conjugated organic molecules. Because the symmetric charge transfer and change in quadrupole moment appear to be important, for molecules with small ground-state mesomeric quadrupole moments, we reasoned that structural features that could further enhance the change in quadrupole moment upon excitation could be beneficial for enhancing the corresponding transition dipole moments and the magnitude of δ. We therefore examined both theoretically and experimentally molecules in which (i) the conjugation length was increased by inserting phenylene-vinylene or phenylene-butadienylene groups (compounds **3** to **5**) to increase the distance over which charge can be transferred; (ii) electron-accepting cyano groups were attached to the central ring of the bis(styryl)benzene backbone (compound **6**), creating a donor-acceptor-donor (D-A-D) motif, to increase the extent of charge transfer from the ends of the molecule to the center; and (iii) the sense of the symmetric charge transfer was reversed by substituting electron-donating alkoxy donors on all three rings of the bis(styryl)benzene and attaching relatively strongly electron-accepting dicyano vinyl (compound **7**), thiobarbituric acid (compound **8**), or 3-(dicyanomethylidenyl)-2,3-dihydrobenzothiophene-2-ylidenyl-1,1-dioxide (compound **9**) groups on both ends, creating acceptor-donor-acceptor (A-D-A) compounds. Finally, we were interested in introducing heavy atoms (for example, bromine atoms, compound **10**) with a large spin-orbit coupling to facilitate intersystem crossing from the S_1 state to the lowest excited triplet state, T_1, aiming to create a two-photon–absorbing molecule that could act as an efficient triplet sensitizer.

We performed the same INDO-MRD-CI calculations described above on a series of model compounds (**3′** to **7′**) for **3** to **7** wherein alkyl groups on amino or alkoxy moieties and phenyl groups on terminal amino moieties were replaced by methyl groups. The results (Table 1) support our proposed design strategies. Increasing the conjugation length of the molecule or increasing the extent of symmetrical charge transfer from the ends of the molecule to the middle, or vice versa, results in a large increase of δ and a shift of the two-photon absorption peak to longer wavelength relative to that of *E*-stilbene.

We synthesized **3** to **10** by standard techniques and characterized them by nuclear magnetic resonance, electronic absorption, fluorescence and mass spectroscopies, and elemental analysis (the details of which will be described elsewhere). The two-photon absorption cross sections of these molecules were measured with the two-photon fluorescence excitation method with nanosecond (*14*) and femtosecond (*7*) laser pulses. In both cases, measurements were performed with fluorophores with well-characterized δ values as reference standards (*7*). The positions and magnitudes of the two-photon resonances, the fluorescence quantum yields, and positions of the one-photon absorption bands are shown in Table 1.

Several important conclusions can be drawn from the data in Table 1: (i) There is good agreement between the peak values of δ measured with femtosecond and nanosecond pulses and calculated with the INDO-MRD-CI method. (ii) The INDO-MRD-CI calculations reproduce the trends in the evolution of the position of the two-photon absorption peak (although, as expected, the absolute excitation energies are systematically overestimated by theory, in part because of overcorrelation of the ground state with the MRD-CI scheme). (iii) Increasing the length of the molecule results in a substantial increase in δ, as can be seen by comparing results for **3**, **4**, and **5** with **2**. (iv) Our hypothesis that D-A-D and A-D-A compounds should have enhanced δ is borne out by the observation of large δ values, in the range of 620×10^{-50} to 4400×10^{-50} cm^4 s photon^{-1}, for **6** to **9** relative to bis-1,4-(2-methylstyryl)benzene, for which δ is 55×10^{-50} cm^4 s photon^{-1} (*15*). (v) There are substantial shifts of the peak position of the two-photon absorption to longer wavelength upon increasing both the conjugation length and the extent of symmetric charge transfer. (vi) Compounds **3**, **4**, **6**, and **7** have very high fluorescence quantum yields, indicating that they could be of interest as fluorescent probes for two-photon microscopy. (vii) The dibromo-substituted

Table 1. Calculated and experimental two-photon excitation cross sections (δ) and peak positions (TPA λ_{max}) for compounds in this work. Experimental δ values determined with nanosecond pulses and femtosecond pulses (given in parentheses) are reported. The uncertainty in the experimental δ values is estimated to be ±15%. Also reported are single-photon absorption maxima (λ_{max}), the wavelengths for fluorescence emission maxima (emission λ_{max}), and the fluorescence quantum yields (Φ_f). For the theoretical results, **1′** to **7′** are model compounds for **1** to **7**, wherein alkyl groups on amino or alkoxy moieties and phenyl groups on terminal amino moieties were replaced by methyl groups.

Theoretical results			Experimental results					
Compound	TPA λ_{max} (nm)	δ (10^{-50} cm^4 s photon^{-1})	Compound	TPA λ_{max} (nm)	δ (10^{-50} cm^4 s photon^{-1})	λ_{max} (nm)	Emission λ_{max} (nm)	Φ_f
1′	466	27.3	**1**	514 (*8*)	12 (*8*)			
2′	529	202.4	**2**	605 (<620)	210 (110 at 620 nm)	374	410	0.90
3′	595	680.5	**3**	730 (~725)	995 (635)	408	455	0.88
4′	599	670.3	**4**	730 (~725)	900 (680)	428	480	0.88
5′	620	712.5	**5**	775 (~750)	1250 (1270)	456	509	0.12
6′	625	950.0	**6**	835 (810)	1940 (3670)	472	525	0.86
7′	666	570.4	**7**	825 940 (815) (910)	480 620 (650) (470)	513	580	0.82
–	–	–	**8**	970	1750	554	641	0.06
–	–	–	**9**	975 (945)	4400* (3700)	618	745	0.0085
–	–	–	**10**	~800	450	424	490	0.41

*There is a large uncertainty in this δ value because of a large uncertainty in the rather low value of Φ_f, which is 0.0055(± 45%). The raw $\Phi_f\delta$ product determined with nanosecond pulses for this compound is 37.5×10^{-50} cm^4 s photon^{-1}, and that determined with femtosecond pulses is 31.5×10^{-50} cm^4 s photon^{-1}. In the table, we report the upper estimate of Φ_f and the value of δ based on it, which gives the more conservative estimate for δ. The values of δ obtained with the average Φ_f (based on determinations in different laboratories) are 6800×10^{-50} cm^4 s photon^{-1} (for nanosecond pulses) and 5700×10^{-50} cm^4 s photon^{-1} (for femtosecond pulses).

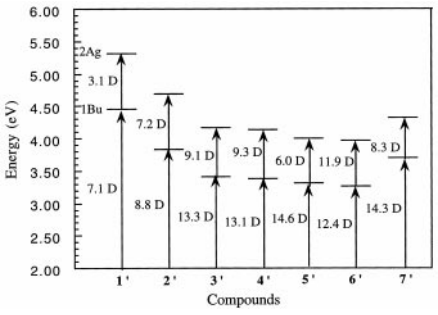

Fig. 2. Scheme of the calculated energy levels and transition dipole moments (in debyes) for the three lowest singlet states for compounds **1′** to **7′** (which are model compounds for **1** to **7**, wherein alkyl groups on amino or alkoxy moieties and phenyl groups on terminal amino moieties were replaced by methyl groups).

compound **10** has a reasonably large δ value, and its fluorescence quantum yield is low in comparison with **3**, consistent with efficient intersystem crossing. Preliminary results indicate that **10** is a singlet O_2 sensitizer, which makes it a good candidate for cytotoxicity and photodynamic therapy studies in biological tissues (*16*).

We suggest that π-conjugated molecules with large changes of quadrupole moment upon excitation are worthy of examination as molecules with large two-photon absorption cross sections. Molecules derived from the design strategies described should greatly facilitate a variety of applications of two-photon excitation in biology, medicine, three-dimensional optical memory, photonics, (*17*) optical limiting (*2*), and materials science (*17*).

References and Notes

1. W. Denk, J. H. Strickler, W. W. Webb, *Science* **248**, 73 (1990); R. M. William, D. W. Piston, W. W. Webb, *FASEB J.* **8**, 804 (1994); W. Denk and K. Svoboda, *Neuron* **18**, 351 (1997); R. H. Köhler, J. Cao, W. R. Zipfel, W. W. Webb, M. R. Hansen, *Science* **276**, 2039 (1997).
2. J. E. Ehrlich *et al.*, *Opt. Lett.* **22**, 1843 (1997).
3. A. A. Said *et al.*, *Chem. Phys. Lett.* **228**, 646 (1994); G. S. He, R. Gvishi, P. N. Prasad, B. Reinhardt, *Opt. Commun.* **117**, 133 (1995).
4. D. A. Parthenopoulos and P. M. Rentzepis, *Science* **245**, 843 (1989); J. H. Strickler and W. W. Webb, *Opt. Lett.* **16**, 1780 (1991).
5. W. Denk, *Proc. Natl. Acad. Sci. U.S.A.* **91**, 6629 (1997).
6. R. R. Birge, *Acc. Chem. Res.* **19**, 138 (1986).
7. C. Xu and W. W. Webb, *J. Opt. Soc. Am. B* **13**, 481 (1996); C. Xu *et al.*, *Proc. Natl. Acad. Sci. U.S.A.* **93**, 10763 (1996).
8. R. J. M. Anderson, G. R. Holtom, W. M. McClain, *J. Chem. Phys.* **70**, 4310 (1979).
9. M. J. S. Dewar, E. G. Zoebisch, E. F. Healy, J. J. P. Stewart, *J. Am. Chem. Soc.* **107**, 3902 (1985).
10. J. Ridley and M. Zerner, *Theoret. Chim. Acta* **32**, 111 (1973).
11. R. J. Buenker and S. D. Peyerimhoff, *ibid.* **35**, 33 (1974).
12. B. Dick, R. M. Hochstrasser, H. P. Trommsdorff, in *Nonlinear Optical Properties of Organic Molecules and Crystals*, D. S. Chemla and J. Zyss, Eds. (Academic Press, Orlando, FL, 1987), vol. 2, pp. 167–170.
13. B. J. Orr and J. F. Ward, *Mol. Phys.* **20**, 513 (1971).
14. The two-photon absorption cross sections were determined by two-photon–excited fluorescence measurements, with 5-ns, 10-Hz pulses from a Nd:yttrium-aluminum-garnet–pumped optical parametric oscillator-amplifier system. The setup consisted of two arms to allow relative measurements with respect to bis-1,4-(2-methylstyryl)benzene (in cyclohexane), fluorescein (in pH 11 water), and rhodamine B (in methanol). The sample chromophores were dissolved in toluene (10^{-4} M concentration); an approximately collimated beam was used to excite the samples over the 1-cm length of the cuvettes. The fluorescence emitted at right angles to the excitation was collected and focused onto photomultiplier tube detectors. The intensity of the incident beam was adjusted to assure excitation in the intensity-squared regime.
15. S. M. Kennedy and F. E. Lytle, *Anal. Chem.* **58**, 2643 (1986). We scaled the peak δ value reported in this paper by a factor chosen to match the long-wavelength data reported therein with that of (*7*).
16. M. Lipson, M. Levin, S. R. Marder, J. W. Perry, unpublished results.
17. B. H. Cumpston *et al.*, in preparation.

18. Support from the NSF (Chemistry Division), Office of Naval Research, and the Air Force Office of Scientific Research (AFOSR) and its Defense University Research Instrumentation Program at the California Institute of Technology is gratefully acknowledged. The research described in this paper was performed in part by the Jet Propulsion Laboratory, California Institute of Technology, as part of its Center for Space Microelectronics Technology, and was supported by the Ballistic Missile Defense Organization, Innovative Science and Technology Office and AFOSR through an agreement with NASA. The work in Mons was carried out within the framework of the Belgium Prime Minister Office of Science Policy "Pôle d'Attraction Interuniversitaire en Chimie Supramoléculaire et Catalyse" PAI 4/11 and is partly supported by the Belgium National Fund for Scientific Research (FNRS-FRFC) and an IBM-Belgium Academic Joint Study; D.B. is a Chercheur Qualifié FNRS, and T.K. is a Ph.D. grant holder of Fund for Research in Industry and Agriculture. The femtosecond two-photon fluorescence excitation cross-section measurements were carried out in the Developmental Resource for Biophysical Imaging Opto-electronics at Cornell University with support of NIH–National Center of Research Resources and NSF. G.S. acknowledges support from the NASA-JOVE program.

7 May 1998; accepted 31 July 1998

Detection and Modeling of NonTidal Oceanic Effects on Earth's Rotation Rate

Steven L. Marcus, Yi Chao, Jean O. Dickey, Pascal Gegout

Subdecadal changes in Earth's rotation rate, and hence in the length of day (LOD), are largely controlled by variations in atmospheric angular momentum. Results from two oceanic general circulation models (OGCMs), forced by observed wind stress and heat flux for the years 1992 through 1994, show that ocean current and mass distribution changes also induce detectable LOD variations. The close similarity of axial oceanic angular momentum (OAM) results from two independent OGCMs, and their coherence with LOD, demonstrate that global ocean models can successfully capture the large-scale circulation changes that drive OAM variability on seasonal and shorter time scales.

Changes in the rotation rate of the solid Earth (that is, its crust and mantle), typically yield variations in the LOD of about 1 ms over several years (*1*). Earth as a whole conserves its angular momentum (with the exception of tidal torques); LOD variations, in particular, arise largely from compensating changes in atmospheric angular momentum (AAM) carried by zonal (west-to-east) winds (*2, 3*). Remaining discrepancies in the axial budget indicate that other reservoirs also store and release appreciable quantities of angular momentum on these time scales, but these have been less well resolved.

In this study we show that (i) a significant nontidal oceanic signal can be detected in geodetic LOD series and (ii) this contribution of OAM helps to close the global budget on seasonal and shorter time scales. Because the three-dimensional observational data needed to compute OAM directly are not available, we use two OGCM simulations as a proxy for our analysis. These comparisons can provide a valuable check on the realism of the model-derived OAM and may be used to estimate contributions from other angular momentum reservoirs, such as changes in terrestrial and atmospheric water storage.

We consider results from two OGCMs whose dynamical formulations differ considerably: the Modular Ocean Model (*4*) (MOM), based on earlier multilevel models developed at the Geophysical Fluid Dynamics Laboratory (*5*), and a multilayer model based on an early version of the Miami Isopycnal Coordinate Ocean Model (MICOM) (*6*). Both MOM and MICOM are based on the primitive equations of fluid flow that use the Boussinesq and hydrostatic approximations. The major differences between the two models are (i) their vertical coordinate systems: MOM uses geometrical depth beneath a rigid lid and MICOM uses a density-based coordinate with a freely varying surface height; and (ii) their treatment of the surface mixed layer: MOM uses a Richardson-number scheme (*7*) and MICOM uses the Kraus-Turner mixed layer model (*8*). Both models have a horizontal resolution of 2° longitude by 1° latitude and comparable vertical resolution (22 and 12 layers, respectively).

The OGCMs were spun up for 10 years starting from climatological temperature and salinity distributions (*9*), forced with climatological monthly wind stress (*10*) and sea surface temperature and salinity (*9*). The models were then driven with surface wind stress derived from the daily National Center for Environmental Prediction (NCEP) 1000-hPa analysis from 1 January 1992 to 15 December 1994, and heat flux as computed using the bulk formulation described in (*11*);

Jet Propulsion Laboratory, California Institute of Technology, 4800 Oak Grove Drive, Pasadena, CA 91109 USA.